Acta Cryst. (1998). B**54**, 798–808

Distortion of Crystal Structures of Some Co^{III} Ammine Complexes. III. Distortion of Crystal Structure of $[Co(NH_3)_5NO_2]Cl_2$ at Hydrostatic Pressures up to 3.5 GPa

Elena V. Boldyreva,[a,b]* Dmitry Yu. Naumov[a,b] and Hans Ahsbahs[c]

[a]*Institute of Solid State Chemistry, Russian Academy of Sciences, Kutateladze 18, Novosibirsk 128, 630128, Russia,* [b]*Novosibirsk State University, Pirogova 2, Novosibirsk 90, 630090, Russia, and* [c]*Institute of Mineralogy and Materials Science Center, Marburg University, Hans-Meerwein Strasse, 35032 Marburg/Lahn, Germany.*
E-mail: elena@solid.nsk.su

(*Received 19 December 1997; accepted 14 April 1998*)

Abstract

This contribution continues comparative studies on the anisotropy of structural distortion of some Co^{III} ammine complexes induced by various actions [Boldyreva, Kivikoski & Howard (1997*a*). *Acta Cryst.* B**53**, 394–404; Boldyreva, Kivikoski & Howard (1997*b*). *Acta Cryst.* B**53**, 405–414]. Changes in the cell parameters of (*OC*-6-22)-pentaamminenitro-*N*-cobalt(III) dichloride were measured by single-crystal X-ray diffraction at pressures up to 3.5 GPa in a diamond anvil cell (DAC). At several pressures (ambient, 0.24, 0.52, 1.25, 1.91 and 3.38 GPa) a full data collection was carried out, and the atomic coordinates and anisotropic atomic displacement parameters were refined. The anisotropy of structural distortion under pressure was shown to be qualitatively different compared with that on cooling (Boldyreva, Kivikoski & Howard, 1997*b*). The role of the non-covalent interactions, in particular hydrogen bonds, in the anisotropy of structural distortion is discussed.

1. Introduction

Over the past few years more and more studies of crystal structures at high pressures have appeared. These studies have different aims, ranging from simulating geochemical processes to studying the behaviour of drugs, materials or biological structures at high pressures. Structural studies at high pressures are a useful tool to study interatomic interactions in crystals, including non-covalent interactions such as hydrogen bonds (see as examples Katrusiak & Nelmes, 1986; Katrusiak, 1990, 1991*a*,*b*,*c*, 1995; Rauw *et al*., 1996). Studies of the anisotropic distortion of a crystal structure within the same polymorph are no less interesting for this purpose than studies of pressure-induced phase transitions.

In the present contribution we discuss the results of measuring lattice parameters of crystals of $[Co(NH_3)_5NO_2]Cl_2$ at pressures up to 3.5 GPa and of the full structural studies of the same crystals in a DAC at several pressures: ambient, 0.24, 0.52, 1.25, 1.91 and 3.38 GPa. The crystal structure of the title compound is built by $[Co(NH_3)_5NO_2]^{2+}$ complex cations (Fig. 1) and chlorine anions. There are several types of hydrogen bonds in the structure, as well as specific interactions between the NO_2 ligands of the complex cations and the chlorine anions (Boldyreva, Kivikoski & Howard, 1997*b*).

This study is part of a larger project aimed at studying the non-covalent interactions in crystals of nitropentammine cobalt(III) complexes and the role of these interactions in the structural distortions induced by low temperature (Boldyreva, Kivikoski & Howard, 1997*a*,*b*,*c*,*d*), high pressure (Boldyreva *et al.*, 1994, 1996; Boldyreva, Naumov & Ahsbahs, 1997, 1998; Boldyreva, Kuz'mina & Ahsbahs, 1998) and solid-state linkage isomerization (Boldyreva, 1994, 1996, 1997; Boldyreva *et al.*, 1993; Masciocchi *et al.*, 1994). The results were preliminarily reported at the German Seminar on High Pressure Crystallography Techniques, in Rauischholzhausen (1996), the Russian National Conference on the Application of X-rays, Synchrotron Radiation, Neutrons and Electrons for Studies of Materials, in Dubna (1997), the 13th Russian National Seminar on Intermolecular Interactions and Conformations of Molecules, in Tver (1997), and at ECM-97 in Lisbon, Portugal (1997).

2. Experimental

The title compound was synthesized from $[Co(NH_3)_5CO_3](NO_3)$, as described by Mäueler (1981). The crystals were grown at ambient temperature from aqueous solutions.

All diffraction experiments were carried out using a Stoe four-circle diffractometer with software specially adapted for high-pressure data collection (Kutoglu, 1997). Mo $K\alpha$ radiation and a graphite monochromator were used.

The pressure was created in a Merrill–Bassett DAC (Merrill & Bassett, 1974) of the four-screw type suggested by Mao & Bell (1980); the cell has been described by Ahsbahs *et al.* (1993). A methanol–ethanol–water (16:3:1) mixture was used as the pressure-transmitting medium (Piermarini *et al.*, 1973). A single

crystal of $AlPO_4$ was used as the internal standard for pressure measurements (Sowa *et al.*, 1990).

A special procedure was applied for lattice parameter measurements (Hazen & Finger, 1982; Kutoglu, 1997), so that each reflection was measured in eight positions. This allowed the precision in the measurement of lattice parameters to be as good as 0.0006 Å and 0.005°, an order of magnitude better than the previous measurements on a powder sample of the title compound (Boldyreva *et al.*, 1994).

Comparative studies at all the pressures given were carried out for the same crystal in the same orientation in the DAC. All experiments were carried out in the dark or in red light to prevent any possible photochemical reaction. The crystal remained unchanged after being stored in the DAC at high pressure for 1 year; it returned to its initial state after the DAC was unloaded back to ambient pressure. Hydrostatic compressing of the same crystal in the second loading cycle resulted in the same changes in the lattice parameters and atomic coordinates as during the first loading.

To minimize the absorption of X-rays by the DAC the 'fixed φ' method (Finger & King, 1978; Kutoglu, 1997) was applied for data collection. Absorption of the X-rays by an empty DAC was measured experimentally and the results were used to correct the intensities of the reflections (Finger & King, 1978; Ahsbahs, 1987). Since the background was 2θ-dependent, ω scans were used for data collection (Ahsbahs, 1987). The Be background was entirely avoided by using a device in front of the counter, as described by Ahsbahs (1987). This allowed the signal-to-background ratio to improve by up to four times (Ahsbahs, 1987). Additionally, to increase the signal-to-background ratio, the sizes of the 2θ and χ counter apertures were varied with 2θ range (being smaller in the lower 2θ range). The data were collected in the full reciprocal volume allowed by the shadow from the DAC [ω in the range from -39 to 40°, χ in the range from -86 to 96°, 2θ in the range from 3 to 72°, $(2\theta$–$\omega)$ in the range from -39 to 40° at $\varphi = \varphi_0$ and $\varphi = \varphi_0 + 180°$; this gave ~30–40% of the total number of reflections which could be measured without the DAC]. The equivalent reflections were merged. In order to gain the best signal-to-background ratio and as many observable reflections as possible, the data collection was very slow (3 s per point, 120 points per reflection, with 0.01° per step).

All the reflections were collected in a profile mode. The raw diffraction data were processed with the computer program *PROFILE* (Naumov & Boldyreva, 1997). *SHELXL*93 (Sheldrick, 1993) was used for data reduction and structure refinement. *ENVIRON* (Naumov & Boldyreva, 1999) was used for plotting fragments of the crystal structures, analysing the environment of the complex cations in the structure and calculating the interatomic distances and angles. Strain tensors were calculated using the program *TENSOR* of

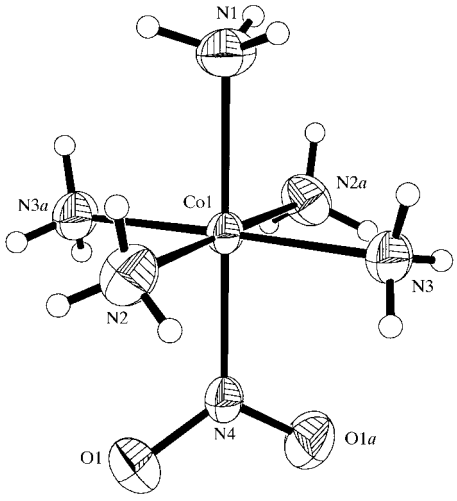

Fig. 1. View of the $[Co(NH_3)_5NO_2]^{2+}$ complex cation showing the labelling of the non-H atoms. Displacement ellipsoids are drawn at 50% probability levels, as at ambient pressure.

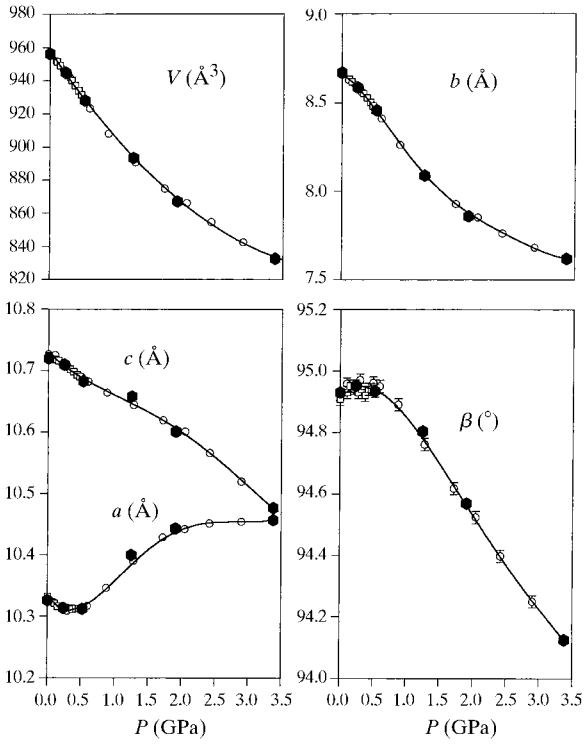

Fig. 2. Changes in lattice parameters and cell volumes of $[Co(NH_3)_5NO_2]Cl_2$ with pressure. ○, points measured in 1996; □, points measured in 1997; ◆, points corresponding to the full structure refinements. Here and in Figs. 3 and 5–12 the lines are 'guides to the eye'. The sizes of the error bars (if not seen) are less than those of the corresponding symbols.

Ohashi, published in the book of Hazen & Finger (1982).

The structures at high pressures were anisotropically distorted compared with those at ambient pressure (Börtin, 1968; Kubota & Ohba, 1992; Boldyreva, Kivikoski & Howard, 1997*c*), but the space group and general structural pattern remained the same. More details on the experimental procedure and structural data are reported elsewhere (Boldyreva, Naumov & Ahsbahs, 1998; Boldyreva, Naumov, Ahsbahs & Kutoglu, 1998).

3. Results and discussion

The changes in lattice parameters and cell volume *versus* pressure are shown in Fig. 2. The data have confirmed, in general, the earlier results obtained by powder diffraction (Boldyreva *et al.*, 1994). Despite the natural overall decrease in volume with increasing pressure, particular directions were shown to expand. The direction of major contraction under pressure coincided with the *b* crystallographic axis; the values of parameters *a* and *c* approached each other at higher pressures. Increased precision of the measurements made it possible to reveal reliably some additional features in the dependence of lattice parameters on pressure compared with an earlier powder diffraction study (Boldyreva *et al.*, 1994), in particular, the pronounced minimum and maximum in the $a(P)$ and $\beta(P)$ curves (Fig. 2). The values of the lattice parameters measured at different pressures were used for calculating the corresponding strain tensors, as described in Hazen & Finger (1982). The values of lattice strain along the principal axes of the strain tensors are plotted in Fig. 3(*a*). The angles of the principal axes with the crystallographic axes changed with pressure; this effect being most pronounced at pressures below ~0.4–0.5 GPa (Fig. 3*b*). In Fig. 4 the orientation of the principal axes of the strain tensor at lower (P = 0.1 GPa) and higher (P = 2.0 GPa) pressures is shown with respect to a fragment of the crystal structure of $[Co(NH_3)_5NO_2]Cl_2$. Treatment of the strain tensors following the procedure described by Garnier, Weigel and co-workers (Garnier *et al.*, 1972; Weigel *et al.*, 1978) has revealed very high values of the aspherism index at all the pressures studied.

Changes in the bond lengths and angles in the complex cations are plotted in Fig. 5. The bonds 'Co—*cis*-NH_3' and 'Co—NO_2' became shorter with the

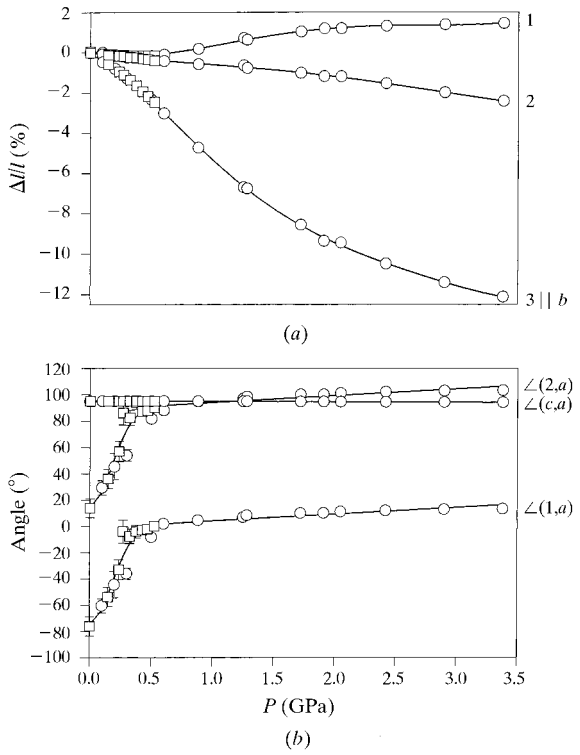

Fig. 3. (*a*) The values of lattice strain along the principal axes 1, 2 and 3 of strain ellipsoids and (*b*) the angles of the principal axes with the crystallographic axes *a* and *c* as a function of pressure; for comparison, the slight changes in the angle between the crystallographic axes *a* and *c* themselves are also plotted. ○, the points measured in 1996; □, the points measured in 1997.

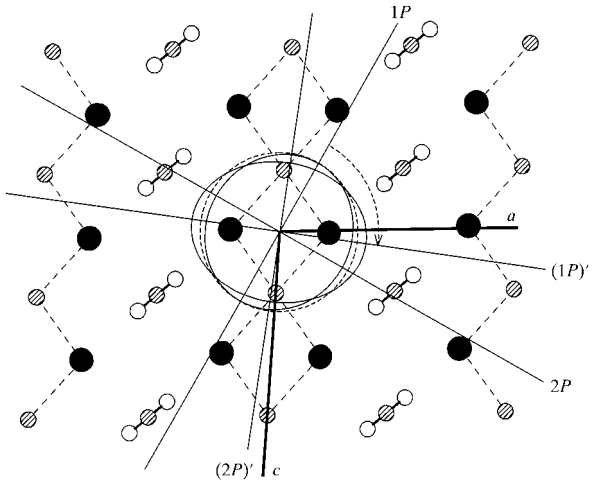

Fig. 4. Orientation of the principal axes of the strain tensor with respect to fragments of the crystal structure of $[Co(NH_3)_5NO_2]Cl_2$ at 0.1 (1*P*, 2*P*) and 2.0 GPa [(1*P*)′, (2*P*)′]. The dashed arrow is a guide to the eye, indicating the rotation of the principal axes of the strain tensor with pressure. The sections of strain ellipsoids at both pressures, as well as the reference sphere at ambient pressure (dashed line), are also plotted; distortion of strain ellipsoids is exaggerated. A layer parallel to the *ac* plane centred at y = 0 is shown. The distances of the atoms from the plane (at ambient pressure) are: Cl^- ±0.1341, *trans*-NH_3 ±0.5000, O ±0.6824, N(NO_2) ±0.0586 Å. Filled circles represent Cl, cross-hatched circles represent N and open circles represent O. The dashed lines show the hydrogen bonds 'NH···Cl^-' between the *trans*-NH_3 ligands and the Cl^- ions. Above and below the layer shown (at distances ~1.8393 Å) there are *cis*-NH_3 ligands also forming hydrogen bonds with the Cl^- ions and with the O atoms of the NO_2 ligands (not shown on the plot). The axes 3*P* and (3*P*)′ are collinear with the *b* crystallographic axis and are perpendicular to the plot plane.

increase in pressure; this contraction being smaller for 'Co—NO_2' bonds. The two types of 'Co—*cis*-NH_3' bonds became more equivalent with the increase in pressure. The bonds 'Co—*trans*-NH_3' first became longer with the increase in pressure and only after the pressure reached ~2 GPa did the bonds start to contract, remaining noticeably longer than the 'Co—*cis*-NH_3' bonds even at ambient pressure. An increase in pressure induced the elongation of 'N—O' bonds and a decrease in the value of the 'O—N—O' angle in the NO_2 ligand at relatively high pressures. It is difficult to make a reliable conclusion on the behaviour of the 'N—O' bond lengths at lower pressures (even a minimum?), since the changes were still small and comparable with

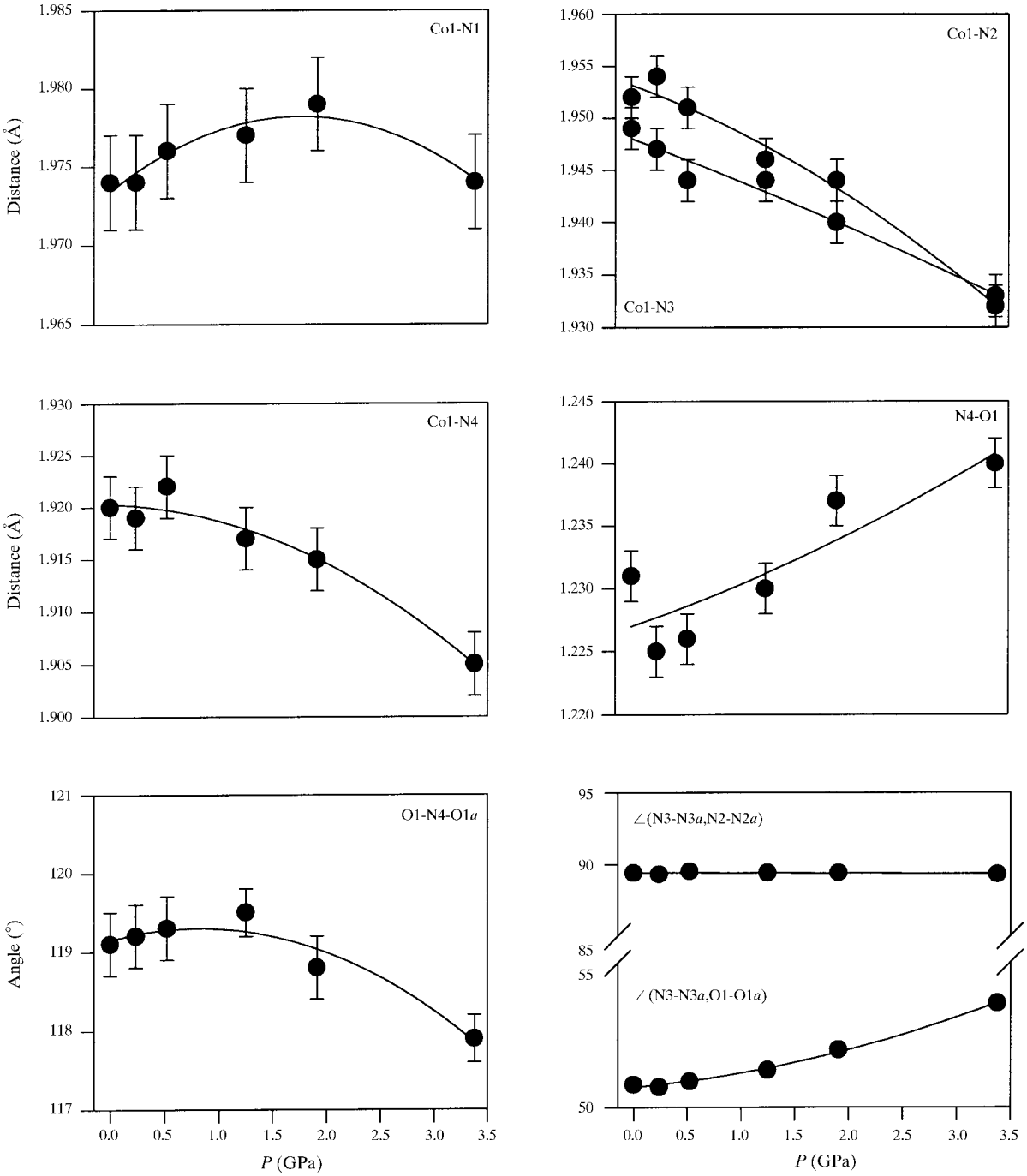

Fig. 5. Changes in bond distances and angles in the complex cation $[Co(NH_3)_5NO_2]^{2+}$ with pressure. The labelling of the atoms is as in Fig. 1.

Table 1. *Selected interatomic distances (Å) in the structure of $[Co(NH_3)_5NO_2]Cl_2$ at different pressures*

No.	*Ai*—*Bj*	0.0001 GPa	0.24 GPa	0.52 GPa	1.25 GPa	1.91 GPa	3.38 GPa
1	N2—Cl1e^{i}	3.348 (2)	3.334 (2)	3.319 (2)	3.274 (2)	3.242 (2)	3.205 (2)
2	N2a^{ii}—Cl1f^{iii}						
3	N3—Cl1c^{iv}	3.353 (2)	3.338 (2)	3.317 (2)	3.274 (2)	3.244 (2)	3.207 (2)
4	N3a^{ii}—Cl1a^{v}						
5	N3—Cl1b^{ii}	3.401 (2)	3.376 (2)	3.354 (2)	3.306 (2)	3.276 (2)	3.230 (2)
6	N3a^{ii}—Cl1						
7	N1—Cl1a^{v}	3.452 (1)	3.444 (1)	3.430 (1)	3.420 (1)	3.407 (1)	3.386 (1)
8	N1—Cl1c^{iv}						
9	N2—Cl1	3.455 (2)	3.444 (2)	3.420 (2)	3.383 (2)	3.356 (2)	3.313 (2)
10	N2a^{ii}—Cl1b^{ii}						
11	N3—Cl1e^{i}	3.463 (2)	3.457 (2)	3.439 (2)	3.414 (2)	3.396 (2)	3.379 (2)
12	N3a^{ii}—Cl1f^{iii}						
13	N1—Cl1	3.477 (1)	3.482 (1)	3.485 (1)	3.515 (1)	3.526 (1)	3.516 (1)
14	N1—Cl1b^{ii}						
15	N2—Cl1d^{vi}	3.516 (2)	3.497 (2)	3.475 (2)	3.432 (2)	3.395 (2)	3.341 (2)
16	N2a^{ii}—Cl1g^{vii}						
17	N3—Cl1g^{vii}	3.792 (2)	3.766 (2)	3.737 (2)	3.672 (2)	3.622 (2)	3.558 (2)
18	N3a^{ii}—Cl1d^{vi}						
19	N2—Cl1c^{iv}	3.873 (2)	3.848 (2)	3.805 (2)	3.697 (2)	3.611 (2)	3.509 (2)
20	N2a^{ii}—Cl1a^{v}						
21	N3—O1c^{viii}	2.972 (2)	2.962 (2)	2.935 (2)	2.889 (2)	2.857 (2)	2.823 (2)
22	O1—N3b^{ix}						
23	N3a^{ii}—O1e^{x}						
24	N3c^{xi}—O1a^{ii}						
25	N2—O1b^{xii}	3.082 (2)	3.053 (2)	3.009 (2)	2.934 (2)	2.871 (2)	2.804 (2)
26	O1—N2b^{i}						
27	N2a^{ii}—O1d^{xiii}						
28	O1a^{ii}—N2c^{iii}						
29	O1—Cl1d^{vi}	3.349 (2)	3.344 (2)	3.332 (2)	3.324 (2)	3.303 (2)	3.263 (2)
30	O1a^{ii}—Cl1g^{vii}						
31	O1—Cl1e^{i}	3.806 (2)	3.804 (2)	3.801 (2)	3.812 (2)	3.810 (2)	3.786 (2)
32	O1a^{ii}—Cl1f^{iii}						
33	N4—Cl1e^{i}	3.775 (1)	3.769 (1)	3.764 (1)	3.779 (1)	3.788 (1)	3.789 (1)
34	N4—Cl1f^{ii}						
35	Cl1c^{iv}—Cl1a^{v}	6.787 (2)	6.777 (2)	6.763 (2)	6.776 (2)	6.772 (2)	6.746 (2)
36	Cl1—Cl1b^{ii}	6.916 (2)	6.931 (2)	6.946 (2)	7.020 (2)	7.047 (2)	7.029 (2)
37	Cl1f^{iii}—Cl1e^{i}	7.549 (2)	7.536 (2)	7.527 (2)	7.557 (2)	7.573 (2)	7.573 (2)
38	Cl1d^{vi}—Cl1g^{vii}	8.617 (2)	8.588 (2)	8.549 (2)	8.504 (2)	8.437 (2)	8.319 (2)
39	Cl1—Cl1d^{vi}	4.176 (1)	4.123 (1)	4.044 (1)	3.862 (1)	3.760 (1)	3.664 (1)
40	Cl1b^{ii}—Cl1g^{vii}						
41	Cl1b^{ii}—Cl1d^{vi}	8.757 (2)	8.728 (2)	8.683 (2)	8.618 (2)	8.559 (2)	8.459 (2)
42	Cl1—Cl1g^{vii}						

Symmetry codes: (i) $\frac{1}{2}-x, \frac{1}{2}+y, \frac{1}{2}-z$; (ii) $-x, y, \frac{1}{2}-z$; (iii) $x-\frac{1}{2}, \frac{1}{2}+y, z$; (iv) $x, -y, \frac{1}{2}+z$; (v) $-x, -y, -z$; (vi) $\frac{1}{2}-x, \frac{1}{2}-y, -z$; (vii) $x-\frac{1}{2}, \frac{1}{2}-y, \frac{1}{2}+z$; (viii) $x, 1-y, \frac{1}{2}+z$; (ix) $x, 1-y, z-\frac{1}{2}$; (x) $-x, 1-y, -z$; (xi) $-x, 1-y, 1-z$; (xii) $\frac{1}{2}-x, y-\frac{1}{2}, \frac{1}{2}-z$; (xiii) $x-\frac{1}{2}, y-\frac{1}{2}, z$.

statistical error. The angles formed by the 'Co—*cis*-NH_3' bonds in the complex cation remained very close to 90 and 180°, whereas the NO_2 ligand rotated noticeably with respect to the lines linking *cis*-NH_3 ligands in the complex cation, so that the corresponding angles deviated more and more from the values of 45° predicted by an *ab initio* calculation for an isolated cation (Boldyreva, unpublished results).

The pressure-induced changes in the interatomic distances of the complex cations were measurable, but too small to account for the large changes observed in the lattice parameters and cell volume. The major contribution to the structural compression was made by changes in the distances between different complex cations, as well as between the complex cations and chlorine anions. The lengths of all the contacts of a complex cation with its environment in the crystal structure at several pressures are summarized in Table 1.† Changes in the '—$NO_2\cdots H_3N$—', '—$NH_3\cdots Cl^{-}$' (hydrogen bonds) and '—$NO_2\cdots Cl^{-}$' distances (another important type of non-covalent interaction in the structure) were of special interest.

The pressure-induced changes in the distances between the NO_2 ligand of a complex cation and the NH_3 ligands of the neighbouring cations are plotted in

† The symmetry codes and labelling of the atoms in Table 1 and in all the figures are the same as were used when considering the anisotropy of the distortion of the same structure on cooling (Boldyreva, Kivikoski & Howard, 1997*b*).

Fig. 6. For comparison, the distances between the NO_2 ligand of a complex cation and *cis*-NH_3 ligands of the same cation (only very slightly pressure-dependent) are shown on the same plot. The two '$—NO_2\cdots H_3N—$' contacts which were longer at ambient pressure shortened noticeably more than the two shorter ones with the increase in pressure, so that at a pressure of ~2.4 GPa the two types of contacts became equal in length and at higher pressures the former shorter contacts became longer and *vice versa*. At ambient pressures the distances between the NO_2 ligand and the *cis*-NH_3 ligands of the same complex cation were shorter than the distances between the same NO_2 ligand and the *cis*-NH_3 ligands of neighbouring cations. The situation changed, however, as the pressure increased. The changes in the '$—NO_2\cdots H_3N—$' intra- and inter-cation distances can be supposed to account for the rotation of the NO_2 ligand with respect to NH_3 ligands in the complex cation (Fig. 5).

The pressure-induced changes in the distances between *trans*-NH_3 ligands and Cl^- anions are plotted in the Fig. 7(*a*). Each *trans*-NH_3 ligand is surrounded in the structure by four Cl^- ions at distances characteristic of hydrogen bonds. The two equivalent '$N(H_3)\cdots Cl$' distances which were shorter at ambient pressure shortened noticeably as the pressure increased, whereas the two equivalent longer ones first expanded and only after ~2 GPa started becoming shorter also. The bands formed by a network of '$—NH_3\cdots Cl^-$' hydrogen bonds in the *c*-crystallographic direction became flatter with increasing pressure – the sum of the 'Cl···N···Cl' angles around the N atom increased and approached 360°

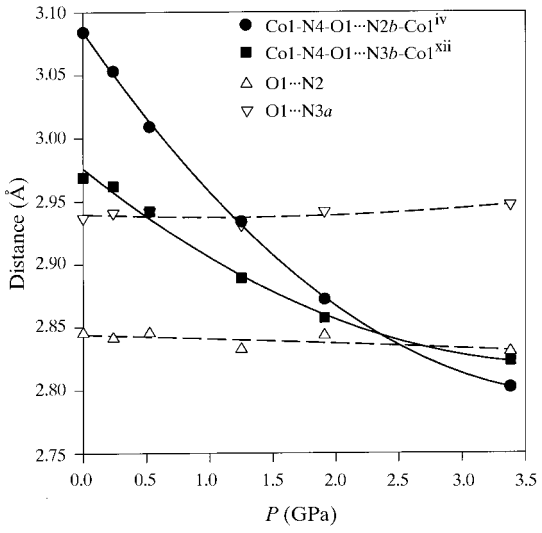

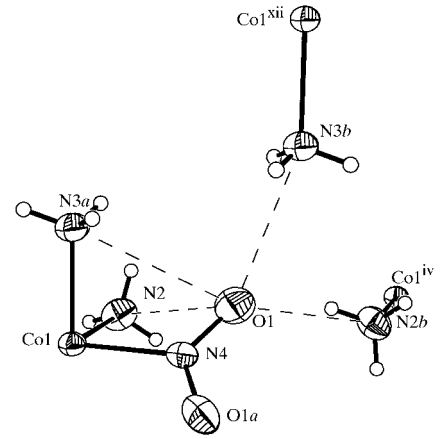

Fig. 6. Changes in the 'N(H)···O' distances with pressure. The scheme below explains the labelling of the atoms. The symmetry codes of the atoms are the same as in Table 1. The symmetry codes for $Co1^{iv}$ and $Co1^{xii}$ are given in the caption to Fig. 11.

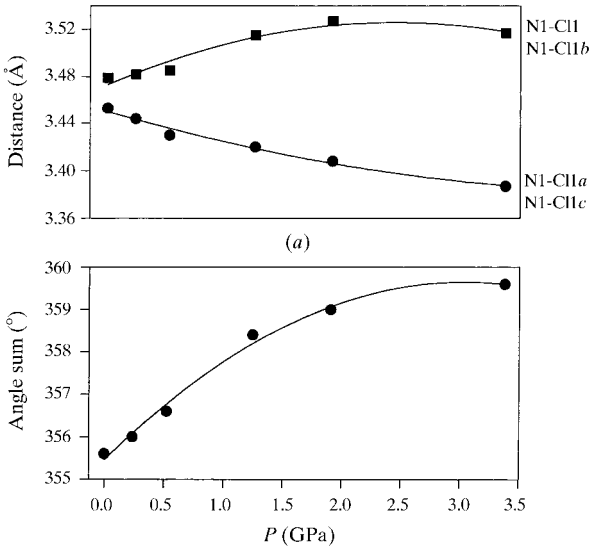

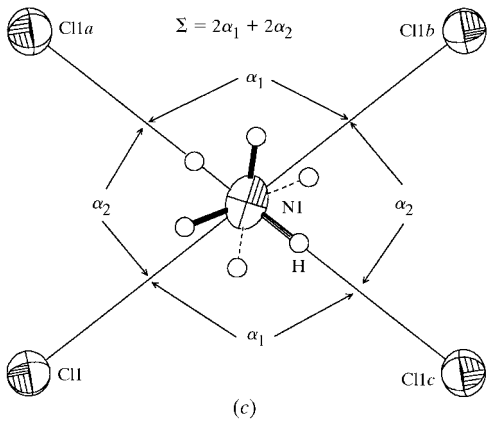

Fig. 7. (*a*) Changes in the '*trans*-N(H)···Cl^-' distances and (*b*) the sum of the 'Cl···N···Cl' angles around *trans*-NH_3 as a function of pressure. The scheme below (*c*) explains the labelling of the atoms. The symmetry codes of the atoms are given in Table 1.

(Fig. 7*b*). A non-monotonous change in the 'Co—*trans*-NH_3' bond length (Fig. 5) may be a consequence of the participation of the *trans*-NH_3 in the hydrogen bonds with chlorine anions. Examples are known from the literature (Ferraro, 1984) of intramolecular bonds expanding with increasing pressure owing to the shortening of intermolecular contacts of the same atom.

The distances between *cis*-NH_3 ligands and Cl^- anions with pressure decreased monotonously, with similar slopes for different contacts (Fig. 8). It is also remarkable that the changes were very similar to the recently measured pressure-induced shortening of the N···Cl distances in the structure of ND_4Cl (Balagurov *et al.*, 1998).

The distances between N atoms of the NO_2 ligands and Cl^- anions decreased with pressure at relatively small (<0.6 GPa) pressure values and increased at higher pressures (Fig. 9*a*). The shorter distances between O atoms of NO_2 ligands and Cl^- anions decreased linearly with pressure, whereas the changes in the longer 'O···Cl' distances to the chlorine ions located above and below the NO_2 ligand were not monotonous with pressure (Figs. 9*b* and 9*c*).

The pressure-induced changes in the hydrogen-bond lengths and the other distances from the atoms of a complex cation to the atoms of its crystalline environment resulted in the movement of complex cations with respect to each other and with respect to Cl^- anions. Complex cations preserved their orientation with respect to each other, but rotated in a cooperative mode with respect to the crystallographic axes (Fig. 10*a*) and the lines linking chlorine anions which surround a complex cation (Fig. 10*b*). The Cl^- anions also changed their relative positions in the structure (Figs. 10*b* and 11*a*). The observed pressure-induced changes in the lattice parameters are a manifestation of the changes in the relative positions of the central atoms of the cations, namely the Co^{III} ions (Fig. 11*b*). They result from a complex interplay of numerous non-covalent interactions of various types in the structure. Different types of distances between a complex cation and its neighbours in the structure change differently in different pressure ranges and this accounts for the peculiar non-linear and not always even monotonous changes in the lattice parameters.

The anisotropy of structural distortion of $[Co(NH_3)_5NO_2]Cl_2$ was qualitatively different for the compression resulting from cooling (Boldyreva, Kivi-

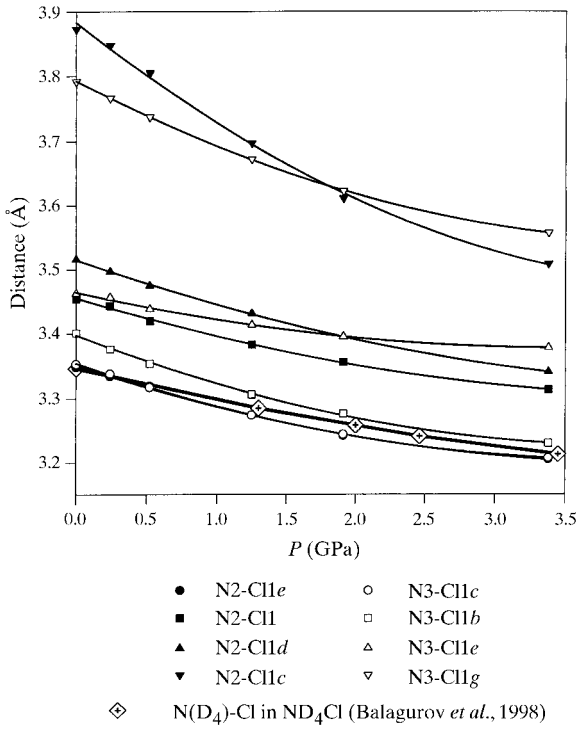

Fig. 8. Changes in the '*cis*-N(H)···Cl^-' distances with pressure. For comparison, the pressure-induced changes in the N(D)···Cl distances in ND_4Cl (Balagurov *et al.*, 1998) are shown in the same plot. The symmetry codes of the atoms are given in Table 1.

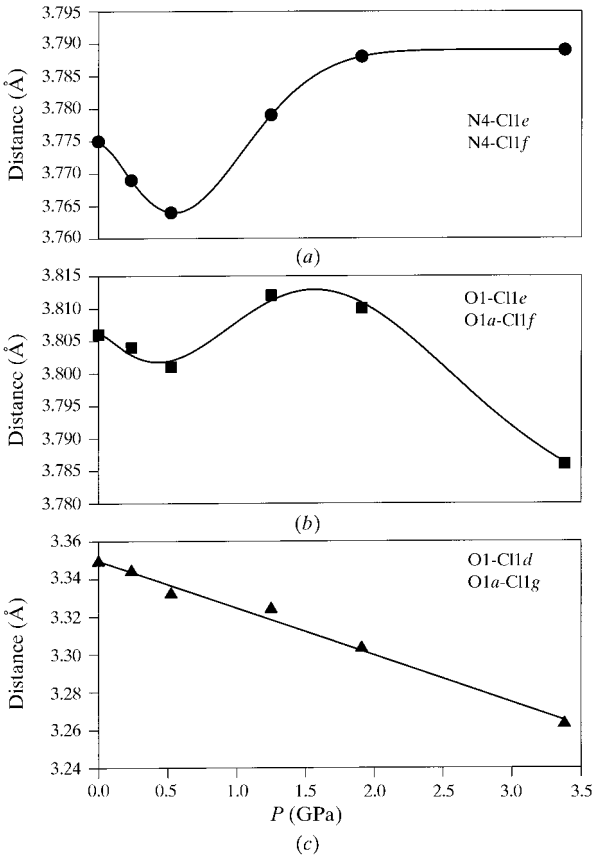

Fig. 9. Changes in (*a*) the 'N(NO_2)···Cl^-' and (*b*) and (*c*) the 'O(NO_2)···Cl^-' distances with pressure. The labelling of atoms is as in the scheme in Fig. 10(*b*). The symmetry codes of the atoms are given in Table 1.

koski & Howard, 1997*b*) and increasing hydrostatic pressure. The difference can be seen from a comparison of the changes in the lattice parameters. When increasing the pressure, the major contraction of the structure was observed along the crystallographic *b* axis, whereas on cooling the same parameter, *b*, on the contrary, increased. The *a* parameter decreased on cooling, whereas it first decreased with pressure (up to ~0.4 GPa) and then started increasing. Parameter *c* almost did not change on cooling, whereas under pressure it decreased very noticeably. The values of *a* and *c* became more equal under pressure, but this effect was not observed for structural compression on cooling. In Fig. 12 the changes in the lattice parameters *versus* temperature and *versus* pressure are shown on the same plot, which is scaled in such a way that the overall volume changes on cooling and under pressure coincide.

Differences in the anisotropy of structural distortion on cooling and under pressure also manifested themselves in changes in interatomic distances. In Fig. 13 the relative changes in the distances from a complex cation to the atoms in its crystalline environment and also in the 'Cl···Cl' distances are compared for the structural compression on cooling (*a*) and under pressure (*b*) for the same overall volume change. The qualitative difference is obvious. On cooling, the longer '*trans*-NH_3···Cl' hydrogen bonds contracted more than the shorter ones (Boldyreva, Kivikoski & Howard, 1997*b*), whereas this was not the case under pressure. Up to 2.0 GPa the longer '*trans*-NH_3···Cl' hydrogen bonds even expanded. In contrast to high pressure, cooling did not make the 'Cl···*trans*-NH_3···Cl' bands flatter; the sum of the 'Cl···N···Cl' angles around a *trans*-NH_3 did not change, although the values of each angle changed quite noticeably. The shorter '$-NO_2\cdots H_3N-$' hydrogen bonds contracted more on cooling than the longer ones, whereas the opposite was true for the compression under pressure. The changes in the distances between N atoms of the NO_2 ligands on cooling and with increasing pressure were also qualitatively different at pressures above 1.0 GPa: they contracted on cooling and expanded with increasing

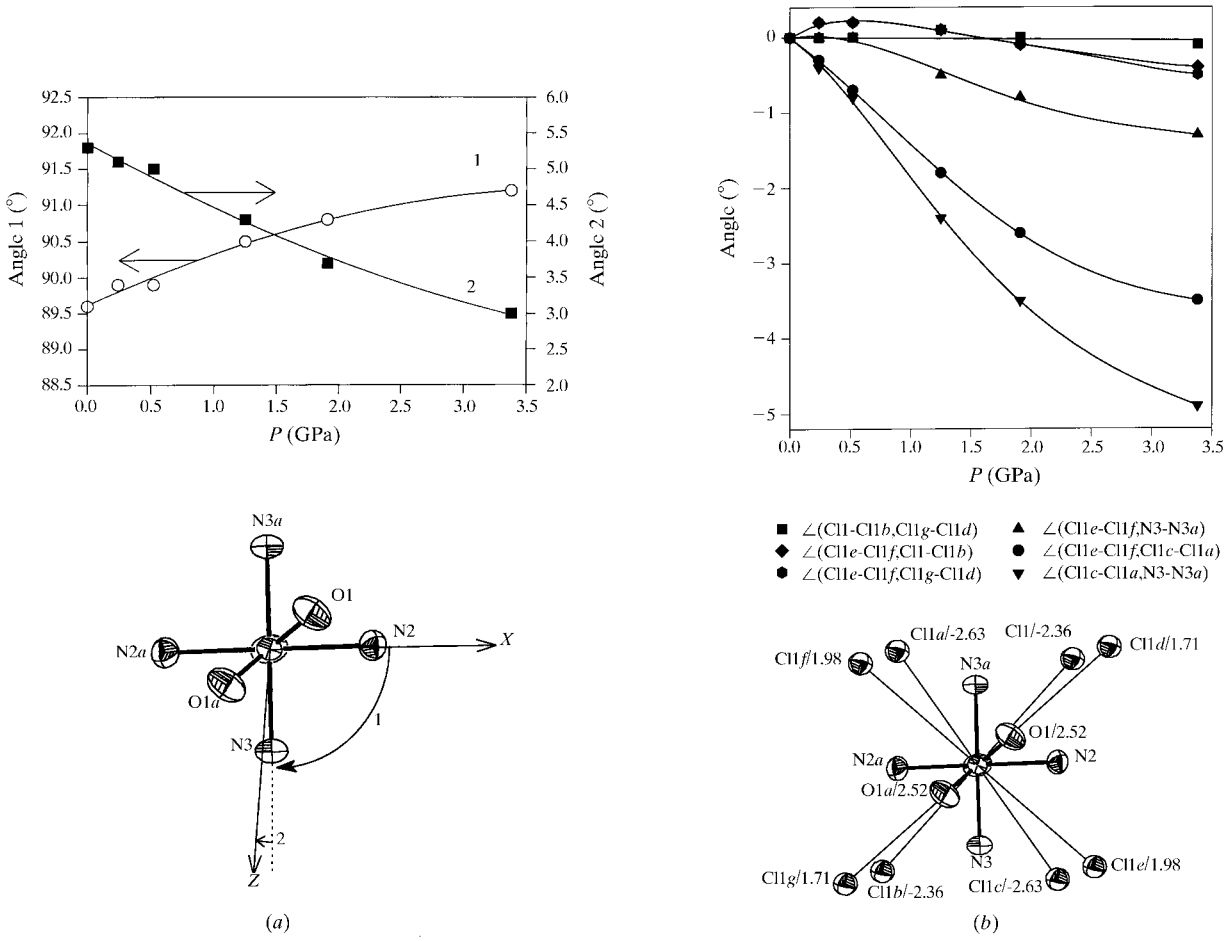

Fig. 10. Rotation of complex cations (*a*) with respect to the crystallographic axes and (*b*) and with respect to the lines linking the Cl^- ions surrounding a complex cation. The schemes below explain the labelling of the atoms. The symmetry codes of the atoms are given in Table 1.

pressure. At lower pressures the '$N(NO_2)\cdots Cl^-$' distances contracted both on cooling and with increasing pressure, but the relative changes in the interatomic distances, corresponding to the same overall volume contraction, were noticeably smaller for pressure-induced compression. The directions of the rotation of the complex cations with respect to the crystallographic axes were also different for structural compression on cooling and with increasing pressure. The changes in the mutual juxtapositions of the Cl^- ions were noticeably different on cooling and under pressure. Structural compression of $[Co(NH_3)_5NO_2]Cl_2$ in the different pressure ranges showed remarkable differences, but in *all* the pressure intervals it was different from the contraction of the same structure on cooling.

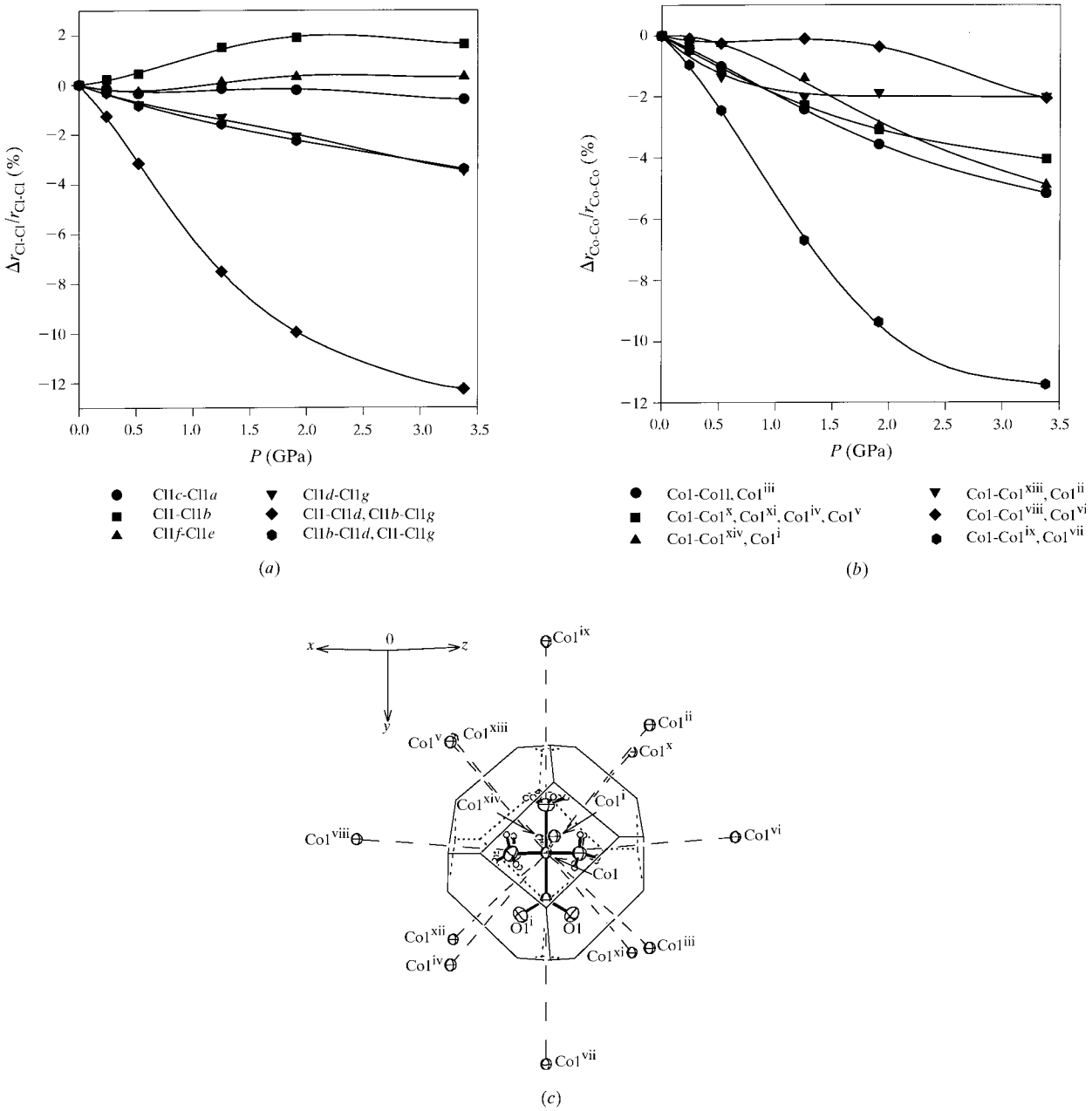

Fig. 11. Changes in (*a*) 'Cl$\cdots$Cl' and (*b*) 'Co$\cdots$Co' distances with pressure. The scheme in (*c*) explains the choice of Co atoms considered as neighbours for a given atom with the help of a Voronoi polyhedron and the labelling of Co atoms. Symmetry codes of the Co atoms: (i) $\frac{1}{2}-x, \frac{1}{2}-y, 1-z$; (ii) $-x, -y, 1-z$; (iii) $-x, 1-y, 1-z$; (iv) $x+\frac{1}{2}, y+\frac{1}{2}, z$; (v) $x+\frac{1}{2}, y-\frac{1}{2}, z$; (vi) $-x-\frac{1}{2}, \frac{1}{2}-y, 1-z$; (vii) $x, 1+y, z$; (viii) $\frac{1}{2}-x, \frac{1}{2}-y, -z$; (ix) $x, y-1, z$; (x) $x-\frac{1}{2}, y-\frac{1}{2}, z$; (xi) $x-\frac{1}{2}, y+\frac{1}{2}, z$; (xii) $-x, 1-y, -z$; (xiii) $-x, -y, -z$; (xiv) $-x-\frac{1}{2}, \frac{1}{2}-y, -z$.

4. Conclusions

A very careful single-crystal X-ray diffraction study of $[Co(NH_3)_5NO_2]Cl_2$ at high hydrostatic pressures up to 3.5 GPa has allowed us to follow the changes in interatomic distances in the structure, which account for the anisotropy of structural distortion. The anisotropy of structural distortion under pressure was shown to be a manifestation of the non-covalent interactions ['$NH_3\cdots Cl^-$' and '$NH_3\cdots O(NO_2)$' hydrogen bonds, '$N(NO_2)\cdots Cl^-$' and '$O(NO_2)\cdots Cl^-$' interactions] in the structure. The same interactions were shown to account for the qualitative difference in structural compression on cooling and under pressure.

The experimental study was carried out at the University of Marburg, where EVB was spending her research term as a Humboldt Fellow. Financial support of the Humboldt Foundation is gratefully acknowledged. The authors are grateful to Dr H. Sowa for providing the single crystal of $AlPO_4$, as well as for many helpful discussions and advice, and to Dr S. Werner for providing a sample of steel for the gasket. The authors are grateful to Dr Ali Kutoglu from Marburg University for his assistance with the software for data collection and helpful discussions. EVB is also grateful to Dr H. Uchtmann and Professor F. Hensel for their hospitality, helpful discussions and assistance in solving various practical problems.

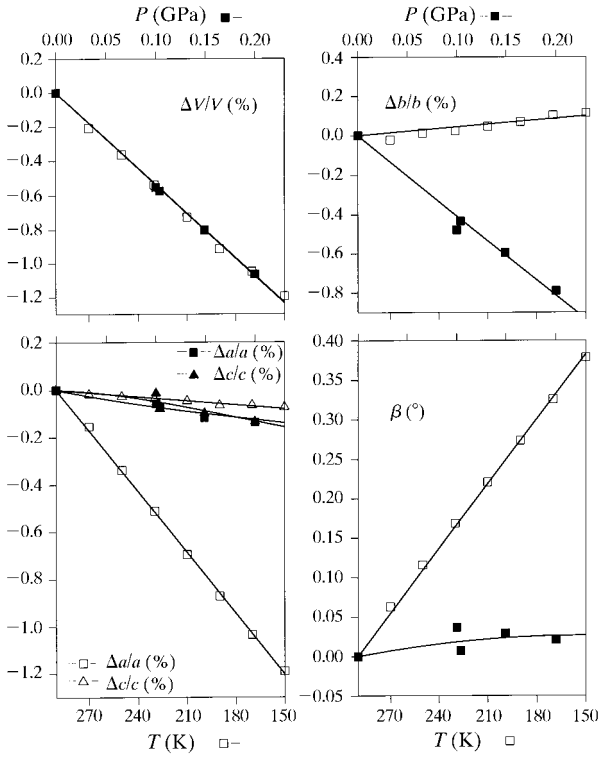

Fig. 12. Comparison of the anisotropy of lattice strain induced in $[Co(NH_3)_5NO_2]Cl_2$ on cooling and by hydrostatic pressure. The changes in volume are the same.

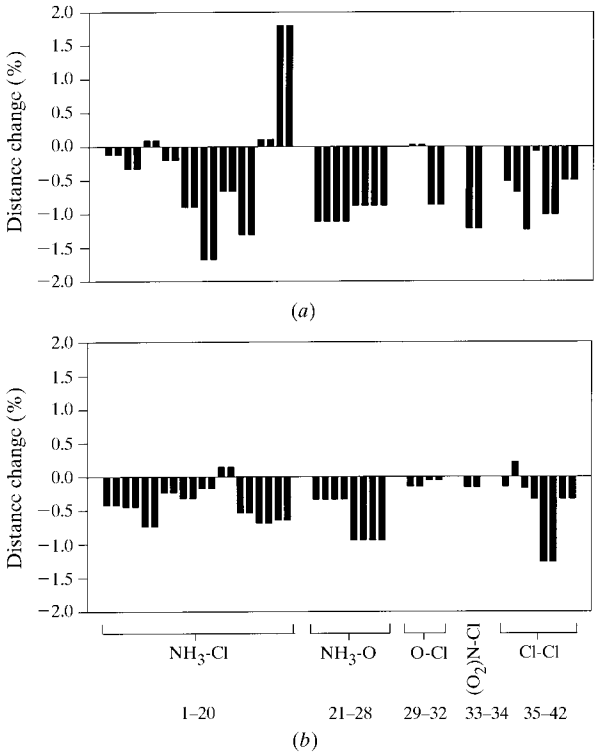

Fig. 13. Changes in the contacts of complex cations with the environment in the crystal structure (*a*) on cooling and (*b*) under hydrostatic pressure P = 0.24 GPa. The changes in volume are the same ($\Delta V/V = -1.2\%$). Numeration of the contacts and the symmetry codes of the atoms are explained in Table 1 (as in Boldyreva, Kivikoski & Howard, 1997*b*).

References

Ahsbahs, H. (1987). *Prog. Cryst. Growth Charact.* **14**, 263–302.
Ahsbahs, H., Dorwarth, R., Hölzer, K. & Kuhs, W. F. (1993). *Z. Kristallogr.* Suppl. **7**, 3–4.
Balagurov, A. M., Kozlenko, D. P., Savenko, B. N., Glazkov, V. P. & Somenkov, V. A. (1998). *Fiz. Tverd. Tela (Russ. J. Solid State Phys.)*, **40**, 142–146.
Boldyreva, E. V. (1994). *Mol. Cryst. Liq. Cryst.* **242**, 17–52.
Boldyreva, E. V. (1996). *Reactivity of Solids. Past, Present, Future*, edited by V. Boldyrev, pp. 141–184. IUPAC Series Chemistry for the 21st Century. Oxford: Blackwell.
Boldyreva, E. V. (1997). *Solid State Ion.* **101–103**, 843–849.
Boldyreva, E. V., Ahsbahs, H. & Naumov, D. Yu. (1996). *Z. Kristallogr.* Suppl. **11**, 76.
Boldyreva, E. V., Ahsbahs, H. & Uchtmann, H. (1994). *Ber. Bunsenges. Phys. Chem.* **98**, 738–745.
Boldyreva, E. V., Kivikoski, J. & Howard, J. A. K. (1997*a*). *Acta Cryst.* B**53**, 394–404.
Boldyreva, E. V., Kivikoski, J. & Howard, J. A. K. (1997*b*). *Acta Cryst.* B**53**, 405–414.

Boldyreva, E. V., Kivikoski, J. & Howard, J. A. K. (1997*c*). *Acta Cryst.* C**53**, 523–526.
Boldyreva, E. V., Kivikoski, J. & Howard, J. A. K. (1997*d*). *Acta Cryst.* C**53**, 526–528.
Boldyreva, E. V., Kuz'mina, S. L. & Ahsbahs, H. (1998). *Zh. Strukt. Khim.* **39**, 424–432.
Boldyreva, E. V., Naumov, D. Yu. & Ahsbahs, H. (1997). *Proceedings of the Russian National Conference on the Application of X-rays, Synchrotron Radiation, Neutrons and Electrons for Studies of Materials (Dubna)*, p. 28. Dubna: United Institute of Nuclear Research.
Boldyreva, E. V., Naumov, D. Yu. & Ahsbahs, H. (1998). *Zh. Strukt. Khim*. **39**, 433–447.
Boldyreva, E. V., Naumov, D. Yu., Ahsbahs, H. & Kutoglu, A. (1998). *Acta Cryst.* C**54**, 1378–1383.
Boldyreva, E. V., Virovets, A. V., Burleva, L. P., Dulepov, V. E. & Podberezskaya, N. V. (1993). *Zh. Strukt. Khim.* **34**, 129–138.
Börtin, O. (1968). *Acta Chem. Scand.* **22**, 2890–2898.
Ferraro, J. R. (1984). *Vibrational Spectroscopy at High External Pressures (The Diamond Anvil Cell)*. New York: Academic Press.
Finger, L. W. & King, H. (1978). *Am. Mineral*. **63**, 337–342.
Garnier, P., Calvarin, G. & Weigel, D. (1972). *J. Chim. Phys. Biol.* **11–12**, 1711–1718.
Hazen, R. M. & Finger, L. W. (1982). *Comparative Crystal Chemistry*. New York: Wiley.
Katrusiak, A. (1990). *Acta Cryst.* B**46**, 246–256.
Katrusiak, A. (1991*a*). *Cryst. Res. Technol.* **26**, 523–531.
Katrusiak, A. (1991*b*). *High Press. Res.* **6**, 155–167.
Katrusiak, A. (1991*c*). *High Press. Res.* **6**, 265–275.
Katrusiak, A. (1995). *Acta Cryst.* B**51**, 873–879.
Katrusiak, A. & Nelmes, R. J. (1986). *J. Phys. C*, **19**, L765–L772.
Kubota, M. & Ohba, S. (1992). *Acta Cryst.* B**48**, 627–632.
Kutoglu, A. (1997). *MDIF*4. *A Program for High-Pressure Data Collection with a Stoe Four-Circle Diffractometer*. Marburg University, Germany.
Mao, K. H. & Bell, P. M. (1980). *Carnegie Inst. Washington Yearb.* **79**, 409–411.
Masciocchi, N., Kolyshev, A. N., Dulepov, V. E., Boldyreva, E. V. & Sironi, A. (1994). *Inorg. Chem.* **33**, 2579–2585.
Mäueler, G. (1981). *Prax. Naturwiss. Teil* 3, **3**, 81–86.
Merrill, L. & Bassett, W. A. (1974). *Rev. Sci. Instrum.* **45**, 290–294.
Naumov, D. Yu. & Boldyreva, E. V. (1997). *Proceedings of the Russian National Conference on the Application of X-rays, Synchrotron Radiation, Neutrons and Electrons for Studies of Materials (Dubna)*, p. 608. Dubna: United Institute of Nuclear Research.
Naumov, D. Yu. & Boldyreva, E. V. (1999). *Zh. Strukt. Khim*. In the press.
Piermarini, G. J., Block, S. & Barnett, J. D. (1973). *J. Appl. Phys.* **44**, 5377–5382.
Rauw, W., Ahsbahs, H., Hitchman, M. A., Lukin, S., Reinen, D., Schultz, J., Simmons, C. J. & Stratemeir, H. (1996). *Inorg. Chem.* **35**, 1902–1911.
Sheldrick, G. M. (1993). *SHELXL*93. *Program for the Refinement of Crystal Structures*. University of Göttingen, Germany.
Sowa, H., Macavei, J. & Schulz, H. (1990). *Z. Kristallogr.* **192**, 119–136.
Weigel, D., Beguemsi, T., Garnier, P. & Berar, J. F. (1978). *J. Solid State Chem.* **23**, 241–251.